EurJIC European Journal of Inorganic Chemistry

ChemPubSoc Europe

FULL PAPER

DOI:10.1002/ejic.201300038

# Synthesis, Structures, and Properties of Diiron Azadithiolate Complexes Containing a Subphthalocyanine Moiety as Biomimetic Models for [FeFe]-Hydrogenases

**Li-Cheng Song,*[a] Fei-Xian Luo,[a] Hao Tan,[a] Xiao-Jing Sun,[a] Zhao-Jun Xie,[a] and Hai-Bin Song[a]**

**Keywords:** Enzyme models / Metalloenzymes / Hydrogenases / Iron / Sulfur / Subphthalocyanine

The first two model compounds for [FeFe]-hydrogenases that contain a subphthalocyanine (SubPc) macrocycle, namely, [{(μ-$SCH_2)_2N(CH_2)_2CO_2$-3-$C_6H_4S_2C_6H_4$-3′-O(SubPc)}$Fe_2(CO)_6$] (**5**) and [{(μ-$SCH_2)_2NC_6H_4$-4-O(SubPc)}$Fe_2(CO)_6$] (**8**), have been synthesized and structurally characterized. The treatment of chlorosubphthalocyanine (SubPc-Cl, **1**) with (3-$HOC_6H_4S)_2$ in toluene gave the corresponding phenoxy-substituted SubPc derivative 3-$HOC_6H_4S_2C_6H_4$-3′-O(SubPc) (**2**) in 78 % yield, whereas the reaction of in-situ-generated [(μ-$HOCH_2S)_2Fe_2(CO)_6$] (**3**) with β-alanine afforded diiron complex [{(μ-$CH_2S)_2N(CH_2)_2CO_2H$}$Fe_2(CO)_6$] (**4**) in 53 % yield. Further treatment of **2** with **4** in the presence of *N*,*N*′-dicyclocarbodiimide (DCC) and *N*,*N*-dimethyl-4-aminopyridine (DMAP) in $CH_2Cl_2$ resulted in the formation of model compound **5** in 86 % yield. Model compound **8** could be prepared by two methods. One method involves the reaction of in-situ-generated **3** with 4-aminophenol in tetrahydrofuran (THF) to give diiron complex [{(μ-$CH_2S)_2NC_6H_4$OH-4}$Fe_2(CO)_6$] (**6**) in 61 % yield and further treatment of SubPc-Cl (**1**) with **6** in toluene to give **8** in 13 % yield. The other method involves the reaction of SubPc-Cl (**1**) with silver triflate (AgOTf) followed by treatment of the resulting intermediate SubPc-OTf (**7**) with **6** in the presence of $Et_3N$ to produce **8** in a much higher yield (59 %). All the new precursors (**2**, **4**, and **6**) and the model compounds **5** and **8** have been fully characterized by elemental analysis and various spectroscopy techniques, as well by X-ray crystallography for **2**, **4**, **6**, and **8**. In addition, the photoinduced $H_2$ production catalyzed by model **8** was preliminarily investigated.

## Introduction

[FeFe]-Hydrogenases are natural metalloenzymes in many microbes and can catalyze the reversible reduction of protons to hydrogen with rapid rates.[1] X-ray crystallographic[2] and IR spectroscopic[3] studies revealed that the active site of [FeFe]-hydrogenases, the so-called H cluster,[4] consists of a dithiolate-bridged butterfly [$Fe_2S_2$] cluster linked to a cubane-like [$Fe_4S_4$] cluster through a single cysteinyl S atom (Figure 1). Structural studies of the active site of [FeFe]-hydrogenases prompted synthetic chemists to prepare a variety of model compounds.[5–10] In recent years, we and others have reported a special type of model compound (so-called light-driven models), in which a photosensitizer (such as a porphyrin, metalloporphyrin, or pyridine-based ruthenium or rhenium complex) is bound to a simple H-cluster model in an attempt to achieve photoinduced $H_2$ production.[9,11–16] However, no light-driven model in which a subphthalocyanine (SubPc) photosensitizer is attached to a simple H cluster has been reported. Therefore, to develop the biomimetic chemistry of [FeFe]-hydrogenases, we decided to design and synthesize two such light-driven models (namely, complexes **5** and **8**, see below) in which the photosensitizer SubPc is attached through an organic chain to the central N atom of an azadithiolate (ADT) ligand in a simple ADT-type model. Subphthalocyanines are regarded as the lower homologues of phthalocyanines. The basic skeleton of these 14 π electron aromatic macrocycles contains three diiminoisoindoline units N-fused around a boron center and they have a $C_3$-symmetrical cone-shaped structure.[17] We utilized SubPc as the photosensitizer for the construction of light-driven models mainly because (i) SubPcs are excellent chromophores with tunable properties for photoinduced electron and/or energy transfer,[18,19] which is closely related to one of the key steps required for hydrogen production catalyzed by natural enzymes, and (ii) SubPcs exhibit strong electronic absorption, high fluorescence quantum yields, small Stokes shifts, and very low reorganization energies,[20,21] which are all fundamental requisites for efficient electron and/or energy transfer and, thus, for efficient photoinduced $H_2$ production. A simple ADT-type model was employed as a catalytic site to construct this type of light-driven model because the dithiolate ligand in the H cluster was recently suggested to be an azadithiolate, in which the central N atom plays an important role

[a] Department of Chemistry, State Key Laboratory of Elemento-Organic Chemistry,
Tianjin 300071, China
E-mail: lcsong@nankai.edu.cn
Homepage: http://www.nankai.edu.cn

for the heterocyclic cleavage or formation of $H_2$ in the enzymatic catalytic process.[22,23] Now, we report the synthesis, structural characterization, and properties of the first two such light-driven model compounds, one with a flexible chain and the other with a rigid chain between the SubPc photosensitizer and the diiron–ADT catalytic site.

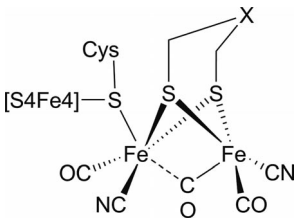


Figure 1. Basic structure of the H cluster determined by protein X-ray crystallography (X = C, N, or O).

## Results and Discussion

### Synthesis and Characterization of the SubPc-Containing ADT-Type Model Compound with a Flexible Organic Chain

To synthesize the SubPc-containing model compound [{(μ-$SCH_2)_2N(CH_2)_2CO_2$-3-$C_6H_4S_2C_6H_4$-3′-O(SubPc)}$Fe_2(CO)_6$] (**5**), we first prepared its two precursors, namely the phenoxy-substituted SubPc derivative 3-$HOC_6H_4S_2C_6H_4$-3′-O(SubPc) (**2**) and the carboxyethyl-substituted diiron complex [{μ-$(SCH_2)_2N(CH_2)_2CO_2H$}$Fe_2(CO)_6$] (**4**). As shown in Scheme 1, the SubPc derivative **2** can be prepared in 78% yield by a condensation reaction of SubPc-Cl (**1**)[24] with 3,3-disulfanediyldiphenol in toluene at reflux, and diiron complex **4** is prepared by a ring-closure reaction of [(μ-$HOCH_2S)_2Fe_2(CO)_6$] (**3**, prepared in situ by the sequential reaction of [(μ-$S_2)Fe_2(CO)_6$] with $Et_3BHLi$, $CF_3CO_2H$, and aqueous $CH_2O$)[25] with β-alanine in tetrahydrofuran (THF) from –78 °C to room temperature in 53% yield. Finally, the expected SubPc-containing ADT model complex **5**, which has a flexible $OC_6H_4S_2C_6H_4$-$O_2C(CH_2)_2$ bridge between its B and N atoms, is obtained in 86% yield by an esterification reaction between the phenol-containing SubPc **2** and the carboxy-containing diiron complex **4** in the presence of *N*,*N*′-dicyclocarbodiimide (DCC) and *N*,*N*-dimethyl-4-aminopyridine (DMAP).

Compounds **2**, **4**, and **5** are air-stable solids and have been fully characterized by various spectroscopic methods and elemental analysis. For example, the $^1H$ NMR spectrum of **2** displays two typical AA′BB′ multiplets at $\delta$ = 7.92–7.94 and 8.87–8.89 ppm for the $H_\beta$ and $H_\alpha$ protons in the SubPc ring,[18,20] whereas **5** exhibited two broad singlets at $\delta$ = 7.85 and 8.81 ppm for its $H_\beta$ and $H_\alpha$ protons. The phenoxy groups attached to the B atoms in **2** and **5** displayed the corresponding signals at $\delta$ = 5.43–6.96 or 5.25–6.85 ppm, respectively. These signals are considerably upfield-shifted owing to shielding by the subphthalocyanine ring current.[26] The $^{13}C$ NMR spectra of **4** and **5** showed signals at $\delta$ = 178.2/207.7 and 168.7/206.6 ppm for their organic and terminal carbonyl groups, respectively. The $^{11}B$ NMR spectra of **2** and **5** displayed singlets at $\delta$ = –14.83 and –14.82 ppm for their respective B atoms.[20] The IR spectra of **2** and **5** exhibited strong absorption bands at ca. 1048 $cm^{-1}$, which are attributed to the B–O stretching vibrations.[18] In addition, precursor **4** and model compound **5** displayed several absorption bands in the range 2072–1975 $cm^{-1}$ for their terminal carbonyl groups.[27]

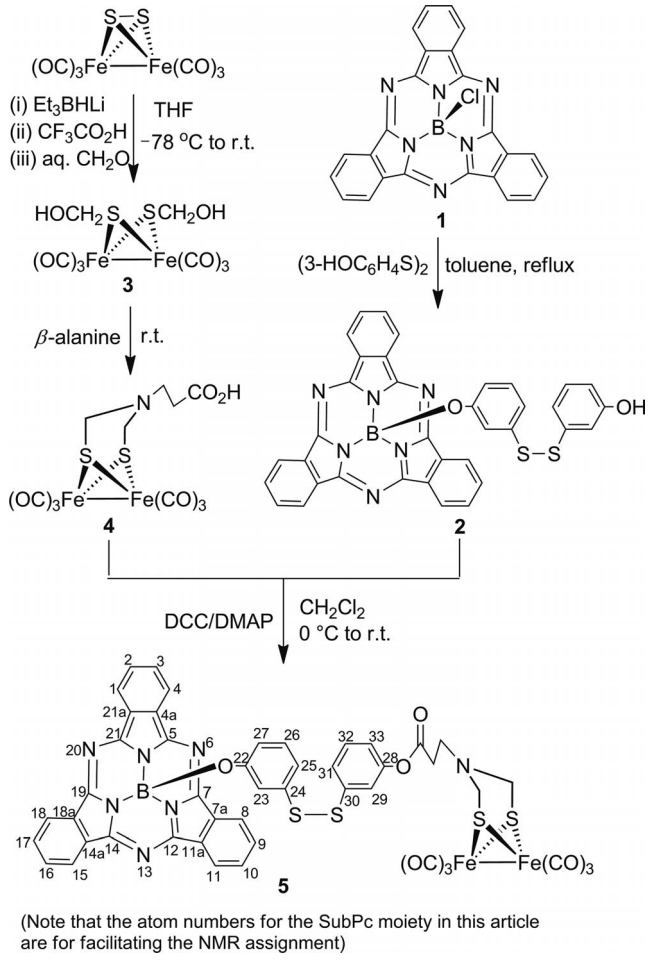


(Note that the atom numbers for the SubPc moiety in this article are for facilitating the NMR assignment)

Scheme 1. Synthetic route to model **5** via **2** and **4**.

Although the crystal structure of model **5** was not determined by X-ray diffraction owing to the lack of suitable single crystals, the single-crystal molecular structures of its precursors **2** and **4** were successfully determined. The ORTEP views of **2** and **4** are shown in Figures 2 and 3, and their selected bond lengths and angles are given in Table 1. The structure of **2** is shown in Figure 2 and is very similar to those of previously reported SubPc derivatives.[26,28–32] The SubPc macrocycle of **2** has a cone-shaped conformation with the tetrahedral boron atom pointing away from the macrocyclic base and the phenoxy group axially bonded to the boron atom. The B–O bond length (1.446 Å), the average B–N bond length (1.489 Å), and the B–O–C bond angle (115.1°) of **2** are comparable with those found in other SubPc derivatives.[33–35] In the structure of **2**, there is an intramolecular hydrogen bond between its phenolic

 

hydroxy group O(2)H(2) and the macrocycle N(3) atom [the bond length and angle of the hydrogen bond O(2)–H(2)···N(3) are 1.964 Å and 178.15°, respectively]. The axial phenoxy group is more tilted toward the macrocycle because of this hydrogen bond and has a B–O–C bond angle of 115.1° and a C(29)–S(1)–S(2)–C(31) torsion angle of 80.72°. The S–S bond length of **2** (2.0261 Å) is actually the same as that of 1,2-bis(3-nitrophenyl) disulfane (2.026 Å)[36] and is very close to that for 1,2-bisphenyl disulfane (2.029 Å).[37]

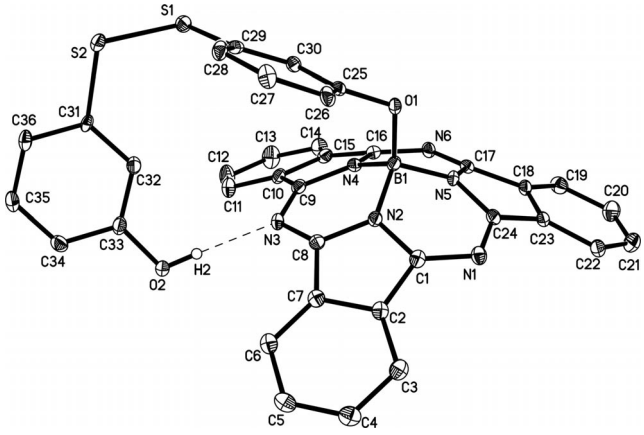


Figure 2. ORTEP view of **2** with 30% probability level ellipsoids.

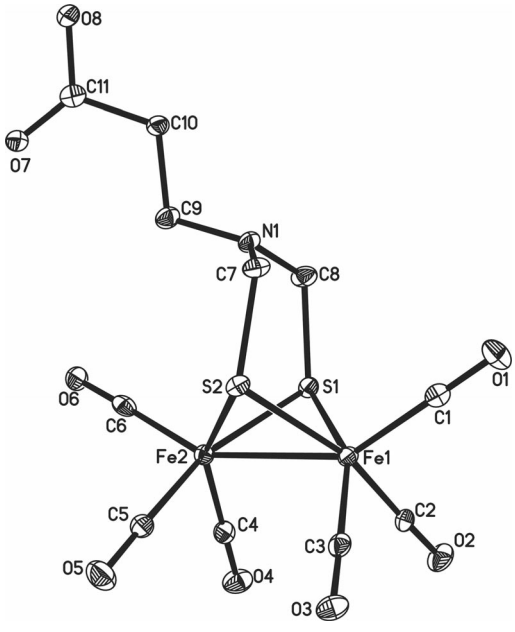


Figure 3. ORTEP view of **4** with 30% probability level ellipsoids.

As can be seen in Figure 3, compound **4** consists of a carboxyethyl-substituted azadithiolate ligand that bridges two $Fe(CO)_3$ units to form two fused six-membered rings. The Fe1S1C8N1C7S2 six-membered ring adopts a chair conformation, whereas the Fe2S2C7N1C8S1 six-membered ring adopts a boat conformation. This complex exists as only one isomer, in which the carboxyethyl functionality is connected to the bridgehead N1 atom by an axial bond.

Table 1. Selected bond lengths [Å] and angles [°] for **2** and **4**.

| | | | |
|---|---|---|---|
| **2** | | | |
| S(2)–C(31) | 1.797(3) | N(4)–B(1) | 1.493(4) |
| S(2)–S(1) | 2.0255(11) | N(5)–B(1) | 1.486(4) |
| S(1)–C(29) | 1.787(3) | N(2)–B(1) | 1.490(4) |
| O(1)–C(25) | 1.385(3) | O(1)–B(1) | 1.446(4) |
| C(9)–N(4)–B(1) | 123.1(2) | O(1)–B(1)–N(2) | 115.3(2) |
| C(25)–O(1)–B(1) | 115.1(2) | N(5)–B(1)–N(2) | 104.9(2) |
| C(17)–N(5)–B(1) | 123.2(3) | N(2)–B(1)–N(4) | 103.6(2) |
| C(1)–N(2)–B(1) | 122.2(3) | C(29)–S(1)–S(2) | 104.22(10) |
| C(8)–N(2)–B(1) | 123.2(3) | C(31)–S(2)–S(1) | 106.91(11) |
| **4** | | | |
| Fe(1)–C(1) | 1.802(5) | Fe(2)–C(6) | 1.809(6) |
| Fe(1)–S(1) | 2.2598(16) | Fe(2)–S(1) | 2.2551(15) |
| Fe(1)–S(2) | 2.2607(14) | Fe(2)–S(2) | 2.2702(15) |
| Fe(1)–Fe(2) | 2.5002(10) | N(1)–C(7) | 1.421(7) |
| S(2)–Fe(1)–Fe(2) | 56.69(4) | S(1)–Fe(1)–S(2) | 84.73(6) |
| S(1)–Fe(2)–S(2) | 84.62(5) | S(1)–Fe(1)–Fe(2) | 56.28(4) |
| S(1)–Fe(2)–Fe(1) | 56.46(4) | Fe(2)–S(1)–Fe(1) | 67.25(5) |
| S(2)–Fe(2)–Fe(1) | 56.33(4) | C(8)–N(1)–C(9) | 120.3(5) |

The Fe1–Fe2 bond length (2.5002 Å) and the sum of the C–N–C bond angles around the N1 atom (253.1°) are very close to those of the other diiron ADT-type model complexes.[38–40]

### Synthesis and Characterization of the SubPc-Containing ADT-Type Model Compound with a Rigid Organic Chain

To examine the influence of the organic bridge between the B atom of the macrocycle and the N atom of the diiron–ADT subsite, we prepared another SubPc-containing light-driven model compound with a rigid $OC_6H_4$ organic chain, namely, model compound [{(μ-$SCH_2$)$_2$N-4-$C_6H_4$O-SubPc}$Fe_2(CO)_6$] (**8**). As shown in Scheme 2, model compound **8** can be prepared by two methods. The first method afforded **8** in low yield (13%) and involves a direct condensation reaction between SubPc-Cl (**1**) and the phenol-containing diiron complex [{(μ-$SCH_2$)$_2$$NC_6H_4$OH-4}$Fe_2(CO)_6$]

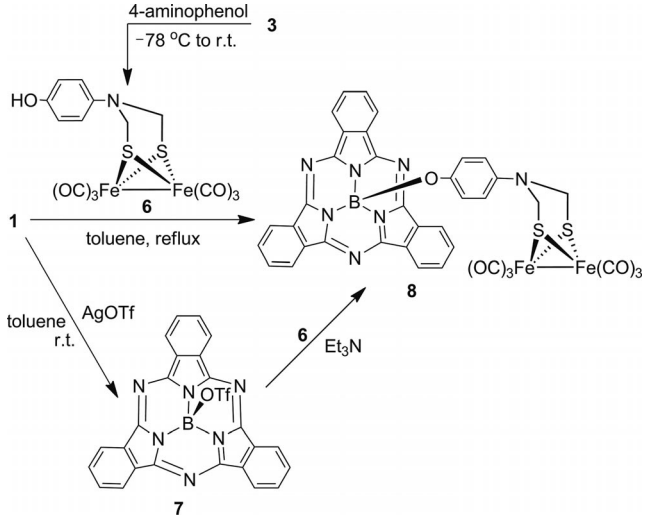


Scheme 2. Synthetic route to model **8** via **6** and **7**.

 

(**6**). Similarly to **4**, complex **6** was prepared in 61% yield by a ring-closure reaction of the in-situ-prepared [(μ-$HOCH_2S)_2Fe_2(CO)_6$] (**3**) with 4-aminophenol in THF from –78 °C to room temperature. The second method has two steps. The first step involves the anion-exchange reaction between SubPc-Cl (**1**) and silver triflate (AgOTf) to give the expected OTf-substituted SubPc derivative **7**.[20] The second step involves the in situ reaction of **7** with diiron complex **6** in the presence of $Et_3N$ to afford **8** in a much higher yield (59%). Notably, the OTf-substituted SubPc derivative **7** was previously reported to be a very reactive intermediate and was characterized in situ by $^1H/^{11}B$ NMR spectroscopy.[20]

Compounds **6** and **8** are also air-stable solids and have been characterized by elemental analysis and various spectroscopic techniques. For example, the $^1H$ NMR spectrum of **6** showed two broad singlets at $\delta$ = 4.25 and 4.58 ppm for its $(CH_2S)_2N$ and OH groups, respectively, and that of **8** displayed two broad singlets at $\delta$ = 7.92 and 8.86 ppm for the $H_\beta$ and $H_\alpha$ protons of its SubPc ring.[18,20] The phenoxy group attached to the B atom in **8** showed two doublets at $\delta$ = 5.39 and 6.14 ppm, which are significantly upfield-shifted for the same reason as those for **2** and **5** indicated above.[26] The $^{13}C$ NMR spectra of **6** and **8** exhibited signals at $\delta \approx$ 207.0 ppm for their terminal carbonyl groups, and the $^{11}B$ NMR spectrum of **8** displayed signals at $\delta$ = –14.81 ppm for its B atom.[20] The IR spectrum of **6** showed a broad band at 3690 $cm^{-1}$ for its OH group and three bands in the range 2074–1964 $cm^{-1}$ for its terminal carbonyl groups, and that of **8** displayed a strong band at 1055 $cm^{-1}$ for its B–O stretching vibration[18] and three bands in the region 2073–1994 $cm^{-1}$ for its terminal carbonyl groups.[27].

The molecular structures of **6** and **8** were unequivocally established by X-ray diffraction analysis. The ORTEP views are depicted in Figures 4 and 5, and Table 2 lists selected bond lengths and angles. As can be seen in Figures 4 and 5, both **6** and **8** contain a diiron–ADT moiety in which the six-membered ring Fe1S2C8N1C7S1 for **6** or Fe2S2C8N7C7S1 for **8** adopts a boat conformation and the six-membered ring Fe2S2C8N1C7S1 for **6** and Fe1S1C7N7C8S2 for **8** are in a chair conformation. The substituted benzene rings are all attached to bridgehead N1 and N7 atoms of **6** and **8** by axial bonds. The Fe1–Fe2 bond lengths of 2.5061 Å for **6** and 2.5047 Å for **8** are very close to those of complex **4** and the other ADT-type model complexes previously reported,[38–40] but they are somewhat shorter than those in the natural enzymes (2.55–2.60 Å).[2a–2c] The sum of the C–N–C bond angles around the bridgehead N1 and N7 atoms increases from 350.7° for **6** to 356.6° for **8**; this is apparently caused by the increased steric repulsion between their SubPc macrocycles and the *cis*-oriented terminal carbonyl groups. The structure of the SubPc macrocycle in **8** is very similar to those of **2** and the previously reported SubPc derivatives.[26,28–32] For example, (i) the SubPc macrocycle has a cone-shaped conformation and the tetrahedral boron atom points away from the macrocyclic base, (ii) the phenoxy substituent is axially bonded to the boron atom, which is coordinated with three nitrogen atoms in a trigonal-pyramidal geometry, and (iii) the B–O bond length (1.423 Å), the average B–N bond length (1.499 Å), and the B–O–C bond angle (119.64°) of **8**

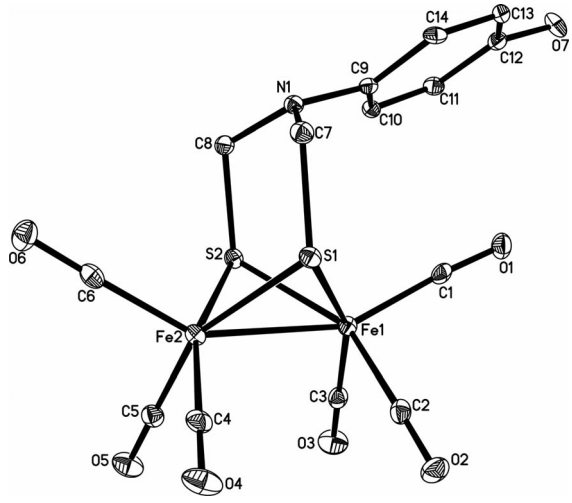


Figure 4. ORTEP view of **6** with 30% probability level ellipsoids.

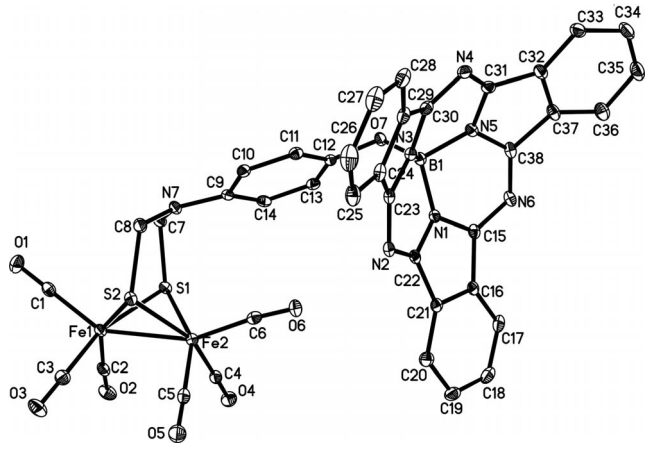


Figure 5. ORTEP view of **8** with 30% probability level ellipsoids.

Table 2. Selected bond lengths [Å] and angles [°] for **6** and **8**.

| | | | |
|---|---|---|---|
| **6** | | | |
| Fe(1)–S(1) | 2.2484(9) | Fe(2)–S(1) | 2.2607(9) |
| Fe(1)–S(2) | 2.2774(9) | Fe(2)–S(2) | 2.2638(9) |
| Fe(1)–Fe(2) | 2.5061(11) | S(1)–C(7) | 1.843(2) |
| N(1)–C(8) | 1.441(3) | S(2)–C(8) | 1.855(2) |
| S(1)–Fe(1)–S(2) | 84.72(4) | C(8)–S(2)–Fe(1) | 113.67(8) |
| S(1)–Fe(2)–Fe(1) | 56.00(3) | Fe(2)–S(2)–Fe(1) | 66.99(3) |
| S(2)–Fe(2)–Fe(1) | 56.77(2) | C(8)–N(1)–C(7) | 113.0(2) |
| Fe(1)–S(1)–Fe(2) | 67.53(3) | C(9)–N(1)–C(7) | 120.0(2) |
| **8** | | | |
| Fe(1)–S(1) | 2.2596(8) | N(1)–B(1) | 1.503(3) |
| Fe(1)–Fe(2) | 2.5047(6) | N(3)–B(1) | 1.494(3) |
| Fe(2)–S(2) | 2.2571(7) | O(7)–B(1) | 1.423(3) |
| Fe(2)–S(1) | 2.2709(8) | N(1)–C(15) | 1.363(3) |
| C(7)–N(7)–C(8) | 114.3(2) | Fe(1)–S(1)–Fe(2) | 67.12(2) |
| S(1)–Fe(1)–S(2) | 84.98(3) | O(7)–B(1)–N(3) | 116.98(19) |
| S(2)–Fe(2)–Fe(1) | 56.53(2) | C(15)–N(1)–B(1) | 122.8(2) |
| S(1)–Fe(2)–Fe(1) | 56.22(2) | N(3)–B(1)–N(1) | 102.5(2) |
| S(1)–Fe(1)–Fe(2) | 56.65(2) | C(12)–O(7)–B(1) | 119.64(19) |

 

are close to those of **2** and some other previously reported SubPc derivatives.[26,28–32] Notably, **8** is the first light-driven model with a SubPc macrocycle covalently linked to a diiron–ADT moiety to be prepared and crystallographically characterized.

### Study on UV/Vis Absorption Spectra and Fluorescence Emission Spectra of 1, 5, and 8

The UV/Vis absorption spectra and fluorescence emission spectra of some SubPc compounds have been investigated.[30,41–44] To understand the photochemical behavior of our model compounds, we determined the UV/Vis absorption spectra and fluorescence emission spectra of **5** and **8** along with those of **1** under the same conditions for comparison. As shown in Figure 6, the UV/Vis spectra of these three compounds all display one Soret band in the range 304–306 nm and two Q bands in the regions 505–507 and 561–563 nm. The Soret and Q bands of **5** and **8** are slightly blueshifted by a maximum of 2 nm relative to the corresponding bands of **1** [For the UV/Vis data of **5** and **8**, see Exp. Sect.; the UV/Vis data of **1** are $\lambda_{max}$ (log$\varepsilon$) = 563 (4.91), 507 (4.35), 306 (4.67) nm]. This implies that axial substitution of the chlorine atom by the phenoxy-attached diiron subunits in **5** and **8** has a negligible influence on their UV/Vis spectra, which are dominated by the very strong π–π* transitions associated with the 14 π electron systems of the SubPc units.[28d,32,43]

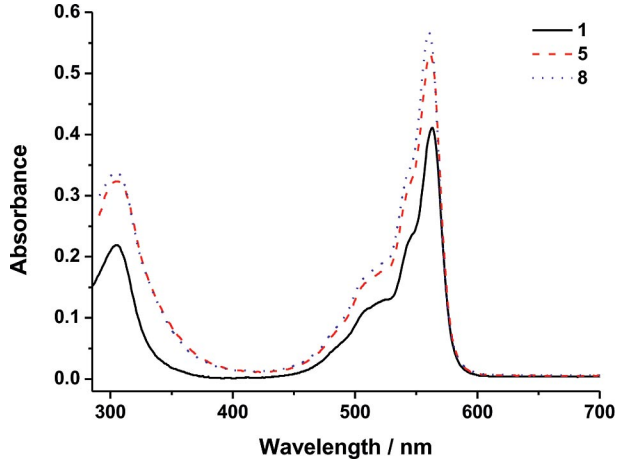


Figure 6. UV/Vis spectra of **1**, **5**, and **8** in THF ($5 \times 10^{-6}$ M).

Axially substituted SubPc derivatives are known to be fluorescent emitters with electron- and/or energy-donating or accepting capabilities.[42–44] As shown in Figure 7, the fluorescence emission spectra of reference compound **1** and model compounds **5** and **8** exhibit fluorescence emission bands at 576, 576, and 575 nm, respectively. Although the three emission bands are almost located at the same position, the band intensities of **5** and **8** are strongly quenched relative to that of **1**; the quenching efficiencies are 68% and 94%, respectively. The remarkable decrease in the intensities of the fluorescence emission bands of **5** and **8** relative to that of **1** could be attributed to strong intramolecular electron transfer (ET) from the photoexcited state of the SubPc macrocycle to the covalently bonded diiron subsite.[9,13,43–45] In addition, the much higher quenching efficiency of model **8** relative to that of **5** demonstrates that the rigid short chain of **8** is much more favorable for intramolecular ET from the SubPc macrocycle to the diiron subsite. Notably, such an intramolecular ET is one of the important steps required for reduction of protons to hydrogen catalyzed by natural enzymes.

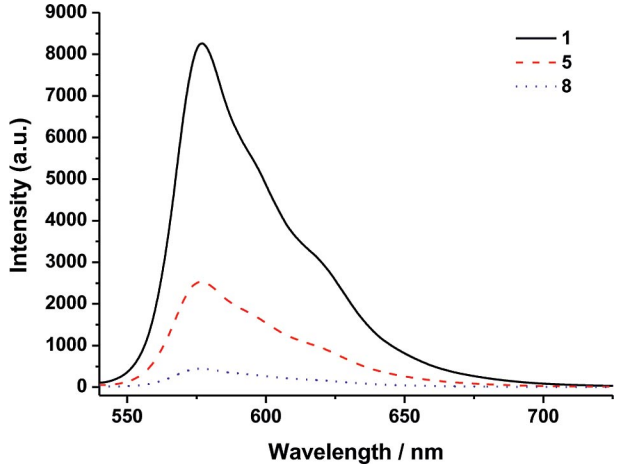


Figure 7. Fluorescence emission spectra ($\lambda_{ex}$ = 530 nm) of **1**, **5**, and **8** in THF ($5 \times 10^{-6}$ M).

### Study on Photoinduced $H_2$ Evolution Under the Action of a Three-Component System Containing Model 8

Catalytic systems for photoinduced $H_2$ evolution usually consist of four separate components: an electron donor, a photosensitizer, a catalyst, and a proton source.[46–50] However, we have recently reported photoinduced $H_2$ evolution by a three-component system. This system comprises an electron donor, a proton source, and a light-driven model that contains a photosensitizer tetraphenylporphyrin moiety attached to a simple ADT-type model for the active site of [FeFe]-hydrogenase.[13,51] To check if our photosensitizer SubPc-containing light-driven models could be act as photoactive catalysts to realize the expected $H_2$ evolution, we chose **8** (as it has a much higher quenching efficiency than **5**) to constitute a three-component system with an electron donor and a proton source for the $H_2$ evolution experiments. It was found that (i) when a 500 W Hg lamp with a UV cutoff filter ($\lambda > 400$ nm) irradiated a THF solution of the three-component system consisting of model **8**, electron donor EtSH, and proton source HOAc, $H_2$ was indeed produced. (ii) As shown in Figure 8, during the first 30 min of irradiation, the $H_2$ evolution increased rapidly, and then became very slow. The reason for fast reduction of the $H_2$ evolution speed could be attributed to decomposition of model **8** under the light irradiation, as the red color of model **8** nearly disappeared after the first 30 min of irradia-

 

tion. A total of 90 min irradiation produced $0.11 \times 10^{-3}$ mmol of $H_2$, which corresponds to a turn over number (TON) of 0.11. (iii) When the same experiment was performed in the absence of any the three components, no $H_2$ evolution was observed. It follows that the presence of electron donor EtSH, proton source HOAc, light-driven model **8**, and light irradiation are essential for such photoinduced $H_2$ evolution.

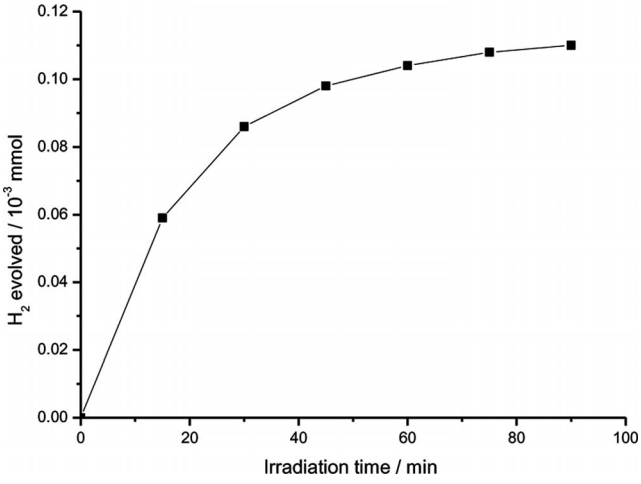


Figure 8. Time dependence of photoinduced $H_2$ evolution from THF solutions (10 mL) consisting of EtSH (10 mM) and HOAc (10 mM) in the presence of model **8** (0.1 mM).

## Summary

We have synthesized and structurally characterized two SubPc-containing light-driven model compounds: one (**5**) with a flexible chain and the other (**8**) with a rigid chain, each bridged between the SubPc B atom and the diiron subunit N atom. In addition, to synthesize **5** and **8**, one SubPc derivative **2** and two diiron complexes **4** and **6** were also prepared and structurally characterized. X-ray crystallographic studies revealed that model **8** consists of a SubPc macrocycle and a diiron–ADT subunit that are axially bonded by a rigid chain to their SubPc B atom and diiron subunit N atom. A comparative study of the fluorescence emission spectra of model compounds **5** and **8** with the reference compound **1** shows that the fluorescence emission bands of **5** and **8** at 576 and 575 nm are strongly quenched relative to that of **1**; the quenching efficiencies are 68 and 94%, respectively. This could be attributed to strong intramolecular ET from the photoinduced SubPc macrocycle to the covalently bonded diiron subunit. In addition, the much higher quenching efficiency of model **8** relative to **5** demonstrates that the rigid short chain in **8** is much more favorable than the flexible long chain in **5** for intramolecular electron transfer. Finally, it should be noted that the catalytic efficiency of model **8** for the photoinduced $H_2$ evolution is very low owing to its severe decomposition. Therefore, the photostability of model **8** should be enhanced to improve its catalytic function under light irradiation. Further studies in this direction will be performed in the near future in this laboratory.

## Experimental Section

**General Comments:** All reactions were performed by using standard Schlenk and vacuum-line techniques under highly prepurified $N_2$. Solvents were distilled under nitrogen by using standard procedures. Chlorosubphthalocyanine (**1**, SubPc-Cl)[52] and [(μ-$S_2$)-$Fe_2(CO)_6$][53] were prepared according to the published methods. Other chemicals such as silver trifluoromethanesulfonate (AgOTf), 4-(dimethylamino)pyridine (DMAP), and *N*,*N*′-dicyclocarbodiimide (DCC) were purchased from commercial suppliers and used without further purification. Preparative TLC was performed on glass plates (26 × 20 × 0.25 cm) coated with silica gel H (10–40 μm). IR spectra were recorded with a Bruker Tensor 27 infrared spectrophotometer. $^1$H, $^{13}$C, and $^{11}$B NMR spectra were recorded with a Bruker Avance 400 NMR spectrometer. Elemental analyses were performed with an Elementar Vario EL analyzer. UV/Vis spectra and fluorescence emission spectra were recorded with a Hitachi U-3900 spectrophotometer and a Hitachi F-4600 spectrophotometer, respectively. Melting points were determined with an X-4 microscopic melting point apparatus.

**3-HO$C_6H_4S_2C_6H_4$-3′-O(SubPc) (2):** A 50 mL Schlenk flask equipped with a magnetic stir-bar, a septum cap, and a reflux condenser topped with a nitrogen inlet tube was charged with SubPc-Cl (0.860 g, 2.00 mmol), 3,3′-disulfanediyldiphenol (1.500 g, 6.00 mmol), and toluene (30 mL). The reaction mixture was heated to reflux for 16 h and then cooled down to room temperature. After removal of the solvent at reduced pressure, the residue was washed with methanol/water (v/v = 4:1) and then subjected to silica gel column chromatography with toluene/THF (v/v = 5:1) as eluent. From the major pink band, **2** was obtained as a pink solid (1.00 g, 78%); m.p. > 250 °C. $^1$H NMR (400 MHz, $CDCl_3$): $\delta$ = 5.43 (dd, $J$ = 2.0, 8.0 Hz, 1 H, 23-H), 5.57 (t, $J$ = 2.0 Hz, 1 H, 27-H), 6.73 (t, $J$ = 8.0 Hz, 1 H, 25-H), 6.96 (d, $J$ = 8.4 Hz, 1 H, 26-H), 7.07 (d, $J$ = 7.2 Hz, 1 H, 29-H), 7.11 (dd, $J$ = 2.0, 8.0 Hz, 1 H, 33-H), 7.32 (t, $J$ = 8.0 Hz, 1 H, 31-H), 7.48 (t, $J$ = 2.0 Hz, 1 H, 32-H), 7.92–7.94, (AA′BB′ system, 6 H, 2-H, 3-H, 9-H, 10-H, 16-H, 17-H), 8.87–8.89 (AA′BB′ system, 6 H, 1-H, 4-H, 8-H, 11-H, 15-H, 18-H) ppm. $^{13}$C NMR (100 MHz, $CDCl_3$): $\delta$ = 112.8, 114.6, 116.4, 116.9 (4 C, C-23, C-27, C-29, C-33), 117.9, 119.6 (2 C, C-25, C-31), 122.0 (6 C, C-1, C-4, C-8, C-11, C-15, C-18), 129.7, 130.0 (2 C, C-26, C-32), 130.1 (6 C, C-2, C-3, C-9, C-10, C-16, C-17), 130.3 (6 C, C-4a, C-7a, C-11a, C-14a, C-18a, C-21a), 136.4, 136.5 (2 C, C-24, C-30), 151.1 (6 C, C-5, C-7, C-12, C-14, C-19, C-21), 153.2, 158.0 (2 C, C-22, C-28) ppm. $^{11}$B NMR (128.3 MHz, $CDCl_3$, $BF_3$·$Et_2O$): $\delta$ = –14.83 (s) ppm. IR (KBr disk): $\tilde{\nu}$ = 3218 (w, O–H), 1584 (s), 1459 (vs), 1435 (s), 1288 (s), 1134 (vs), 1050 (vs, B–O), 764 (s), 741 (vs) cm$^{-1}$. $C_{36}H_{21}BN_6O_2S_2$ (644.5): calcd. C 67.09, H 3.28, N 13.04; found C 67.07, H 3.35, N 12.95.

**[{μ-$(SCH_2)_2N(CH_2)_2CO_2H$}$Fe_2(CO)_6$] (4):** A red solution of [(μ-$S_2$)$Fe_2(CO)_6$] (0.860 g, 2.50 mmol) in THF (30 mL) was cooled to –78 °C and then $Et_3BHLi$ (5.00 mL, 5.00 mmol) was added dropwise to give a green solution containing [(μ-LiS)$_2Fe_2(CO)_6$]. To this solution was added $CF_3CO_2H$ (0.50 mL, 5.00 mmol) and the solution changed immediately from green to red, which indicated the complete conversion of [(μ-LiS)$_2Fe_2(CO)_6$] to [(μ-HS)$_2$Fe$_2$-$(CO)_6$]. The mixture was stirred for another 10 min, and 37% aqueous $CH_2O$ (0.50 mL, 5.00 mmol) was added. The new mixture was warmed to room temperature and stirred at this temperature for

 

1 h to give [(μ-HOCH$_2$S)$_2$Fe$_2$(CO)$_6$]. β-Alanine (0.223 g, 2.50 mmol) was added, and the mixture was stirred at room temperature for 3 h. The solvent was removed under reduced pressure, and the residue was subjected to TLC separation with $CH_2Cl_2$/petroleum ether (v/v = 1:1) as eluent. From the major red band, **4** was obtained as a red solid (0.603 g, 53%); m.p. 125–126 °C. $^1$H NMR (300 MHz, $CDCl_3$): $\delta$ = 2.37 (br. s, 2 H, NCH$_2$C*H*$_2$CO$_2$H), 3.01 (br. s, 2 H, NC*H*$_2$CH$_2$CO$_2$H), 3.56 [br. s, 4 H, (CH$_2$S)$_2$N] ppm. $^{13}$C NMR (100 MHz, $CDCl_3$): $\delta$ = 32.8 (NCH$_2$*C*H$_2$CO$_2$), 52.0 (N*C*H$_2$CH$_2$CO$_2$), 52.7 (SCH$_2$N), 178.2 (C=O), 207.7 (C≡O) ppm. IR (KBr disk): $\tilde{\nu}$ = 2069 (s), 2032 (vs), 2002 (vs), 1991 (vs), 1975 (s, C≡O), 1702 (vs, C=O) cm$^{-1}$. $C_{11}H_9Fe_2NO_8S_2$ (459.0): calcd. C 28.78, H 1.98, N 3.05; found C 28.64, H 2.00, N 3.02.

**[{(μ-SCH$_2$)$_2$N(CH$_2$)$_2$CO$_2$-3-C$_6$H$_4$S$_2$C$_6$H$_4$-3′-O(SubPc)}Fe$_2$(CO)$_6$] (5):** A mixture of the simple ADT-type model [{(μ-SCH$_2$)$_2$N-(CH$_2$)$_2$CO$_2$H}Fe$_2$(CO)$_6$] (**4**, 0.184 g, 0.40 mmol), SubPc derivative **2** (0.130 g, 0.20 mmol), and DMAP (0.024 g, 0.02 mmol) in $CH_2Cl_2$ (30 mL) was stirred at 0 °C for 30 min and then DCC (0.248 g, 1.20 mmol) was added. The mixture was stirred at room temperature for 12 h. The solvent was removed under reduced pressure, and the residue was subjected to TLC separation with $CHCl_3$/ethyl acetate (v/v = 40:1) as eluent. From the major pink band, **5** was obtained as a pink solid (0.186 g, 86%); m.p. > 250 °C. $^1$H NMR (400 MHz, $CDCl_3$): $\delta$ = 2.50 (br. s, 2 H, NCH$_2$C*H*$_2$CO$_2$), 3.09 (br. s, 2 H, NC*H*$_2$CH$_2$*C*O$_2$), 3.60 [br. s, 4 H, (CH$_2$S)$_2$N], 5.25 (br. s, 1 H, 23-H), 5.61 (br. s, 1 H, 27-H), 6.70 (br. s, 2 H, 25-H, 26-H), 6.85 (br. s, 1 H, 29-H), 6.98 (br. s, 1 H, 33-H), 7.10 (br. s, 1 H, 31-H), 7.20 (br. s, 1 H, 32-H), 7.85 (br. s, 6 H, 2-H, 3-H, 9-H, 10-H, 16-H, 17-H), 8.81 (br. s, 6 H, 1-H, 4-H, 8-H, 11-H, 15-H, 18-H) ppm. $^{13}$C NMR (100 MHz, $CDCl_3$): $\delta$ = 32.4 (NCH$_2$*C*H$_2$CO$_2$), 50.9 (N*C*H$_2$CH$_2$CO$_2$), 51.8 (SCH$_2$N), 116.7, 116.8, 118.7, 118.9 (4 C, C-23, C-27, C-29, C-33), 119.3, 123.5 (2 C, C-25, C-31), 121.2 (6 C, C-1, C-4, C-8, C-11, C-15, C-18), 128.3, 128.7 (2 C, C-26, C-32), 128.8 (6 C, C-2, C-3, C-9, C-10, C-16, C-17), 129.9 (6 C, C-4a, C-7a, C-11a, C-14a, C-18a, C-21a), 136.0, 137.9 (2 C, C-24, C-30), 149.6, 152.3 (2 C, C-22, C-28), 150.3 (6 C, C-5, C-7, C-12, C-14, C-19, C-21), 168.7 (C=O), 206.6 (C≡O) ppm. $^{11}$B NMR (128.3 MHz, $CDCl_3$, $BF_3$·$Et_2O$): $\delta$ = –14.82 (s) ppm. IR (KBr disk): $\tilde{\nu}$ = 2072 (s), 2030 (vs), 1993 (vs, C≡O), 1759 (m, C=O), 1584 (m), 1458 (s), 1432 (m), 1287 (m), 1132 (s), 1047 (s, B–O), 763 (m), 741 (s) cm$^{-1}$. UV/Vis (THF): $\lambda_{max}$ (log$\varepsilon$) 562 (5.03), 507 (4.47), 306 (4.81) nm. $C_{47}H_{28}BFe_2N_7O_9S_4$ (1085.6): calcd. C 52.00, H 2.60, N 9.03; found C 52.30, H 2.74, N 9.00.

**[{(μ-SCH$_2$)$_2$NC$_6$H$_4$OH-4}Fe$_2$(CO)$_6$] (6):** The same procedure as that for the preparation of diiron complex **4** was followed. 4-Aminophenol (0.273 g, 2.50 mmol) was added to the in-situ-prepared solution containing [(μ-HOCH$_2$S)$_2$Fe$_2$(CO)$_6$]. Diiron complex **6** (0.730 g, 61%) was isolated as a red solid; m.p. 139–141 °C. $^1$H NMR (400 MHz, $CDCl_3$): $\delta$ = 4.25 [br. s, 4 H, (CH$_2$S)$_2$N], 4.58 (br. s, 1 H, OH), 6.67 (br. s, 2 H, 2*m*-H of NC$_6$H$_4$), 6.82 (br. s, 2 H, 2*o*-H of NC$_6$H$_4$) ppm. $^{13}$C NMR (100 MHz, $CDCl_3$): $\delta$ = 50.6 (SCH$_2$N), 116.7, 118.0 (4 *o,m*-C of C$_6$H$_4$), 139.4, 149.9 (2 *ipso*-C of C$_6$H$_4$), 207.0 (C≡O) ppm. IR (KBr disk): $\tilde{\nu}$ = 3690 (m, O–H), 2074 (s), 2031 (vs), 1964 (vs, C≡O) cm$^{-1}$. $C_{14}H_9Fe_2NO_7S_2$ (479.1): calcd. C 35.16, H 1.89, N 2.92; found C 35.00, H 2.09, N 2.95.

**[{(μ-SCH$_2$)$_2$NC$_6$H$_4$-4-O(SubPc)}Fe$_2$(CO)$_6$] (8):** Method (i): A mixture of SubPc-Cl (0.172 g, 0.40 mmol) and **7** (0.382 g, 0.80 mmol) in toluene (30 mL) was heated to reflux for 16 h. The solvent was removed under reduced pressure, and the residue was subjected to TLC separation with $CHCl_3$/ethyl acetate (v/v = 30:1) as eluent to give **8** (0.046 g, 13%) as a pink solid. Method (ii): A mixture of SubPc-Cl (0.344 g, 0.80 mmol) and AgOTf (0.256 g, 1.00 mmol) was stirred in toluene (30 mL) at room temperature for 2 h. Diiron complex **6** (0.764 g, 1.60 mmol) and triethylamine (0.140 mL, 1.00 mmol) were added, and the mixture was stirred for 2 h. The solvent was then removed under reduced pressure to give a sticky residue. The residue was subjected to TLC separation with $CHCl_3$/ethyl acetate (v/v = 30:1) as eluent. From the major pink band, **8** (0.412 g, 59%) was obtained as a pink solid; m.p. > 250 °C. $^1$H NMR (400 MHz, $CDCl_3$): $\delta$ = 4.07 [s, 4 H, (SCH$_2$)$_2$N], 5.39 (d, *J* = 7.2 Hz, 2 H, 23-H, 27-H), 6.14 (d, *J* = 7.2 Hz, 2 H, 24-H, 26-H), 7.92 (br. s, 6 H, 2-H, 3-H, 9-H, 10-H, 16-H, 17-H), 8.86 (br. s, 6 H, 1-H, 4-H, 8-H, 11-H, 15-H, 18-H) ppm. $^{13}$C NMR (100 MHz, $CDCl_3$): $\delta$ = 50.1 (SCH$_2$N), 116.8 (2 C, C-23, C-27), 120.5 (2 C, C-24, C-26), 122.2 (6 C, C-1, C-4, C-8, C-11, C-15, C-18), 129.9 (6 C, C-2, C-3, C-9, C-10, C-16, C-17), 131.0 (6 C, C-4a, C-7a, C-11a, C-14a, C-18a, C-21a), 139.4, 146.4 (2 C, C-22, C-25), 151.3 (6 C, C-5, C-7, C-12, C-14, C-19, C-21), 206.9 (C≡O) ppm. $^{11}$B NMR (128.3 MHz, $CDCl_3$, $BF_3$·$Et_2O$): $\delta$ = –14.81 (s) ppm. IR (KBr disk): $\tilde{\nu}$ = 2073 (s), 2033 (vs), 1994 (vs, C≡O), 1614 (w), 1459 (s), 1433 (m), 1288 (m), 1253 (s), 1055 (s, B–O), 763 (m), 742 (s) cm$^{-1}$. UV/Vis (THF): $\lambda_{max}$ (log$\varepsilon$) = 561 (5.05), 505 (4.51), 304 (4.83) nm. $C_{38}H_{20}BFe_2N_7O_7S_2$ (873.25): calcd. C 52.27, H 2.32, N 11.23; found C 52.33, H 2.27, N 11.12.

**Photoinduced $H_2$ Evolution Catalyzed by Model 8:** A 30 mL Schlenk flask fitted with a $N_2$ inlet tube, a septum cap, a magnetic stir bar, and a water-cooling jacket was charged with model **8** (0.87 mg, 0.001 mmol), EtSH (7.4 μL, 0.1 mmol), HOAc (5.7 μL, 0.1 mmol), and THF (10 mL). The resulting solution was stirred and thoroughly deoxygenated by bubbling nitrogen through it. The solution was then irradiated at about 25 °C (controlled by the cooling jacket) through a Pyrex filter ($\lambda$ > 400 nm) by using a 500 W Hg lamp. The UV cutoff filter was used to obtain visible light and to avoid decomposition of EtSH.[35] During the photoinduced catalysis, the evolved $H_2$ was withdrawn periodically by using a gas-tight syringe. The $H_2$ was analyzed by gas chromatography with a Shimadazu GC-2014 instrument equipped with a thermal conductivity detector and a carbon molecular sieves column (3 mm × 2.0 m) and with $N_2$ as the carrier gas. The total amount of $H_2$ produced during 90 min of irradiation was $0.11 \times 10^{-3}$ mmol.

**X-ray Structure Determinations of 2, 4, 6, and 8:** Single crystals of **2**, **4**, **6**, and **8** suitable for X-ray diffraction analyses were grown by a slow diffusion of $CH_2Cl_2$ into their hexane solutions at room temperature or at –5 °C. Single crystal of **2**, **6**, or **8** were mounted on a Rigaku MM-007 (rotating anode) diffractometer equipped with a Saturn 724 CCD. Data were collected at 113 K by using a confocal monochromator with Mo-$K_\alpha$ radiation ($\lambda$ = 0.71070 Å) in the $\omega$–$\theta$ scanning mode. Data collection, reduction, and absorption correction were performed with the CRYSTALCLEAR program.[54] A single crystal of **4** was mounted on a Bruker SMART 1000 automated diffractometer. Data were collected at room temperature with graphite-monochromated Mo-$K_\alpha$ radiation (0.71073 Å) in the $\omega$–$\theta$ scanning mode. Absorption correction was performed by the SADABS program.[55] All structures were solved by direct methods by using the SHELXS-97 program[56] and refined by full-matrix least-squares techniques (SHELXL-97)[57] on $F^2$. Hydrogen atoms were located by using the geometric method. Details of crystal data, data collections, and structure refinements are summarized in Table 3.

CCDC-916878 (for **2**), -916879 (for **4**), -916880 (for **6**), and -916881 (for **8**) contain the supplementary crystallographic data for this paper. These data can be obtained free of charge from the Cambridge Crystallographic Data Centre via www.ccdc.cam.ac.uk/data-request/cif.

 

Table 3. Crystal data and structure refinements details for **2**, **4**, **6**, and **8**.

| | **2** | **4** | **6** | **8** |
|---|---|---|---|---|
| Formula | $C_{36}H_{21}BN_6O_2S_2$ | $C_{11}H_9Fe_2NO_8S_2$ | $C_{14}H_9Fe_2NO_7S_2{\cdot}0.5H_2O$ | $C_{38}H_{20}BFe_2N_7O_7S_2{\cdot}2CH_2Cl_2{\cdot}0.5H_2O$ |
| $M_r$ [g mol$^{-1}$] | 644.52 | 459.01 | 488.05 | 1052.10 |
| Crystal system | orthorhombic | monoclinic | triclinic | triclinic |
| $T$ [K] | 113(2) | 113(2) | 113(2) | 113(2) |
| Space group | $Pca2_1$ | $P2_1/c$ | $P\bar{1}$ | $P\bar{1}$ |
| $a$ [Å] | 19.699(3) | 12.627(3) | 6.886(2) | 10.994(2) |
| $b$ [Å] | 12.198(2) | 22.817(5) | 13.812(5) | 11.4951(18) |
| $c$ [Å] | 25.266(4) | 17.139(3) | 18.402(7) | 17.310(3) |
| $\alpha$ [°] | 90 | 90 | 90.385(8) | 80.198(8) |
| $\beta$ [°] | 90 | 95.45(3) | 93.514(8) | 84.881(9) |
| $\gamma$ [°] | 90 | 90 | 90.282(12) | 75.519(9) |
| $V$ [Å$^3$] | 6071.4(18) | 4915.5(17) | 1746.8(11) | 2084.7(6) |
| Z | 8 | 12 | 4 | 2 |
| $\rho_{calcd.}$ [g cm$^{-3}$] | 1.410 | 1.861 | 1.856 | 1.676 |
| $\mu$ [mm$^{-1}$] | 0.221 | 2.064 | 1.941 | 1.115 |
| Crystal size [mm] | 0.20 × 0.18 × 0.12 | 0.18 × 0.16 × 0.12 | 0.20 × 0.18 × 0.10 | 0.20 × 0.18 × 0.10 |
| $F$(000) | 2656 | 2760 | 980 | 1062 |
| Reflections collected | 51722 | 33150 | 17859 | 21372 |
| Independent reflections | 12787 | 8648 | 6129 | 9768 |
| $2\theta_{max}$ [°] | 54.18 | 50.04 | 50.04 | 55.76 |
| $R$ | 0.0524 | 0.0577 | 0.0309 | 0.0349 |
| $R$w | 0.0970 | 0.1207 | 0.0564 | 0.0891 |
| Goodness-of-fit | 1.092 | 1.074 | 0.912 | 1.011 |
| Largest diff. peak and hole [e Å$^{-3}$] | 0.209/–0.278 | 0.592/–0.626 | 0.386/–0.458 | 1.026/–0.628 |

## Acknowledgments

The authors are grateful to the State Key Project of Fundamental Research for Nanoscience and Nanotechnology (973) (grant number 2011CB935902), the National Natural Science Foundation of China (NSFC) (grant numbers 21132001 and 21272122), and the Tianjin Natural Science Foundation (grant number 09JCZDJC27900) for financial support.

[1] a) M. W. W. Adams, E. I. Stiefel, *Science* **1998**, *282*, 1842–1843; b) R. Cammack, *Nature* **1999**, *397*, 214–215; c) Y. Nicolet, C. Cavazza, J. C. Fontecilla-Camps, *J. Inorg. Biochem.* **2002**, *91*, 1–8.

[2] a) J. W. Peters, W. N. Lanzilotta, B. J. Lemon, L. C. Seefeldt, *Science* **1998**, *282*, 1853–1858; b) Y. Nicolet, C. Piras, P. Legrand, E. C. Hatchikian, J. C. Fontecilla-Camps, *Structure* **1999**, *7*, 13–23; c) Y. Nicolet, A. L. De Lacey, X. Vernède, V. M. Fernandez, E. C. Hatchikian, J. C. Fontecilla-Camps, *J. Am. Chem. Soc.* **2001**, *123*, 1596–1601; d) B. J. Lemon, J. W. Peters, *Biochemistry* **1999**, *38*, 12969–12973.

[3] a) A. J. Pierik, M. Hulstein, W. R. Hagen, S. P. J. Albracht, *Eur. J. Biochem.* **1998**, *258*, 572–578; b) A. L. De Lacey, C. Stadler, C. Cavazza, E. C. Hatchikian, V. M. Fernandez, *J. Am. Chem. Soc.* **2000**, *122*, 11232–11233; c) Z. Chen, B. J. Lemon, S. Huang, D. J. Swartz, J. W. Peters, K. A. Bagley, *Biochemistry* **2002**, *41*, 2036–2043.

[4] M. W. W. Adams, *Biochim. Biophys. Acta* **1990**, *1020*, 115–145.

[5] a) For reviews, see for example: C. Tard, C. J. Pickett, *Chem. Rev.* **2009**, *109*, 2245–2274; b) J.-F. Capon, F. Gloaguen, P. Schollhammer, J. Talarmin, *Coord. Chem. Rev.* **2005**, *249*, 1664–1676; c) J. C. Fontecilla-Camps, A. Volbeda, C. Cavazza, Y. Nicolet, *Chem. Rev.* **2007**, *107*, 4273–4303; d) L.-C. Song, *Acc. Chem. Res.* **2005**, *38*, 21–28.

[6] a) F. Gloaguen, J. D. Lawrence, M. Schmidt, S. R. Wilson, T. B. Rauchfuss, *J. Am. Chem. Soc.* **2001**, *123*, 12518–12527; b) C. M. Thomas, T. Liu, M. B. Hall, M. Y. Darensbourg, *Inorg. Chem.* **2008**, *47*, 7009–7024; c) M. Razavet, S. C. Davies, D. L. Hughes, J. E. Barclay, D. J. Evans, S. A. Fairhurst, X. Liu, C. J. Pickett, *Dalton Trans.* **2003**, 586–595; d) L.-C. Song, J. Cheng, J. Yan, H.-T. Wang, X.-F. Liu, Q.-M. Hu, *Organometallics* **2006**, *25*, 1544–1547.

[7] a) H. Li, T. B. Rauchfuss, *J. Am. Chem. Soc.* **2002**, *124*, 726–727; b) J.-F. Capon, S. Ezzaher, F. Gloaguen, F. Y. Pétillon, P. Schollhammer, J. Talarmin, *Chem. Eur. J.* **2008**, *14*, 1954–1964; c) G. Si, W.-G. Wang, H.-Y. Wang, C.-H. Tung, L.-Z. Wu, *Inorg. Chem.* **2008**, *47*, 8101–8111.

[8] a) L.-C. Song, Z.-Y. Yang, H.-Z. Bian, Y. Liu, H.-T. Wang, X.-F. Liu, Q.-M. Hu, *Organometallics* **2005**, *24*, 6126–6135; b) L.-C. Song, Z.-Y. Yang, Y.-J. Hua, H.-T. Wang, Y. Liu, Q.-M. Hu, *Organometallics* **2007**, *26*, 2106–2110.

[9] L.-C. Song, M.-Y. Tang, F.-H. Su, Q.-M. Hu, *Angew. Chem.* **2006**, *118*, 1148; *Angew. Chem. Int. Ed.* **2006**, *45*, 1130–1133.

[10] J. Windhager, M. Rudolph, S. Bräutigam, H. Görls, W. Weigand, *Eur. J. Inorg. Chem.* **2007**, 2748–2760.

[11] F. Wang, W.-G. Wang, H.-Y. Wang, G. Si, Z.-H. Tung, L.-Z. Wu, *ACS Catal.* **2012**, *2*, 407–416.

[12] L.-C. Song, M.-Y. Tang, S.-Z. Mei, J.-H. Huang, Q.-M. Hu, *Organometallics* **2007**, *26*, 1575–1577.

[13] L.-C. Song, L.-X. Wang, M.-Y. Tang, C.-G. Li, H.-B. Song, Q.-M. Hu, *Organometallics* **2009**, *28*, 3834–3841.

[14] A. M. Kluwer, R. Kapre, F. Hartl, M. Lutz, A. L. Spek, A. M. Brouwer, P. W. N. M. van Leeuwen, J. N. H. Reek, *Proc. Natl. Acad. Sci. USA* **2009**, *106*, 10460–10465.

[15] L.-C. Song, L.-X. Wang, B.-S. Yin, Y.-L. Li, X.-G. Zhang, Y.-W. Zhang, X. Luo, Q.-M. Hu, *Eur. J. Inorg. Chem.* **2008**, 291–297.

[16] J. S. Lindsey, I. C. Schreiman, H. C. Hsu, P. C. Kearney, A. M. Marguerettaz, *J. Org. Chem.* **1987**, *52*, 827–836.

[17] C. G. Claessens, D. González-Rodríguez, T. Torres, *Chem. Rev.* **2002**, *102*, 835–853.

[18] D. González-Rodríguez, M. V. Martínez-Díaz, J. Abel, A. Perl, J. Huskens, L. Echegoyen, T. Torres, *Org. Lett.* **2010**, *12*, 2970–2973.

[19] a) A. Medina, C. G. Claessens, G. M. A. Rahman, A. M. Lamsabhi, O. Mo, M. Yáñez, D. M. Guldi, T. Torres, *Chem. Commun.* **2008**, 1759–1761; b) D. González-Rodríguez, L. Echegoyen, E. Carbonell, D. M. Guldi, T. Torres, *Angew. Chem.* **2009**, *121*, 8176; *Angew. Chem. Int. Ed.* **2009**, *48*, 8032–8036.

 

[20] J. Guilleme, D. González-Rodríguez, T. Torres, *Angew. Chem.* **2011**, *123*, 3568; *Angew. Chem. Int. Ed.* **2011**, *50*, 3506–3509.
[21] R. A. Kipp, J. A. Simon, M. Beggs, H. E. Ensley, R. H. Schmehl, *J. Phys. Chem. A* **1998**, *102*, 5659–5664.
[22] a) Y. Nicolet, B. J. Lemon, J. C. Fontecilla-Camps, J. W. Peters, *Trends Biochem. Sci.* **2000**, *25*, 138–143; b) Y. Nicolet, A. L. Lacey, X. Vernède, V. M. Fernandez, E. C. Hatchikian, J. C. Fontecilla-Camps, *J. Am. Chem. Soc.* **2001**, *123*, 1596–1601.
[23] H. Fan, M. B. Hall, *J. Am. Chem. Soc.* **2001**, *123*, 3828–3829.
[24] A. Meller, A. Ossko, *Monatsh. Chem.* **1972**, *103*, 150–155.
[25] J. L. Stanley, T. B. Rauchfuss, S. R. Wilson, *Organometallics* **2007**, *26*, 1907–1911.
[26] H. Xu, X.-J. Jiang, E. Y. M. Chan, W.-P. Fong, D. K. P. Ng, *Org. Biomol. Chem.* **2007**, *5*, 3987–3992.
[27] J. P. Collman, L. S. Hegedus, J. R. Norton, R. G. Finke, *Principles and Applications of Organotransition Metal Chemistry*, 2nd ed., University Science Books, Mill Valley, **1987**.
[28] a) C. G. Claessens, T. Torres, *J. Am. Chem. Soc.* **2002**, *124*, 14522–14523; b) D. González-Rodríguez, T. Torres, D. M. Guldi, J. Rivera, M. Á. Herranz, L. Echegoyen, *J. Am. Chem. Soc.* **2004**, *126*, 6301–6313; c) D. González-Rodríguez, T. Torres, M. M. Olmstead, J. Rivera, M. Á. Herranz, L. Echegoyen, C. A. Castellanos, D. M. Guldi, *J. Am. Chem. Soc.* **2006**, *128*, 10680–10681; d) P. V. Solntsev, K. L. Spurgin, J. R. Sabin, A. A. Heikal, V. N. Nemykin, *Inorg. Chem.* **2012**, *51*, 6537–6547.
[29] C. Romero-Nieto, A. Medina, A. Molina-Ontoria, C. G. Claessens, L. Echegoyen, N. Martín, T. Torres, D. M. Guldi, *Chem. Commun.* **2012**, *48*, 4953–4955.
[30] H. Xu, D. K. P. Ng, *Chem. Asian J.* **2009**, *4*, 104–110.
[31] a) H. Zhu, S. Shimizu, N. Kobayashi, *Angew. Chem.* **2010**, *122*, 8172; *Angew. Chem. Int. Ed.* **2010**, *49*, 8000–8003; b) G. E. Morse, A. S. Paton, A. Lough, T. P. Bender, *Dalton Trans.* **2010**, *39*, 3915–3922.
[32] M. E. El-Khouly, J. B. Ryu, K.-Y. Kay, O. Ito, S. Fukuzumi, *J. Phys. Chem. C* **2009**, *113*, 15444–15453.
[33] A. S. Paton, G. E. Morse, A. J. Lough, T. P. Bender, *CrystEngComm* **2011**, *13*, 914–919.
[34] H. Xu, D. K. P. Ng, *Inorg. Chem.* **2008**, *47*, 7921–7927.
[35] T. Fukuda, M. M. Olmstead, W. S. Durfee, N. Kobayashi, *Chem. Commun.* **2003**, 1256–1257.
[36] D. Cannon, C. Glidewell, J. N. Low, J. L. Wardell, *Acta Crystallogr., Sect. C* **2000**, *56*, 1267–1268.
[37] A. L. Fuller, L. A. S. Scott-Hayward, Y. Li, M. Bühl, A. M. Z. Slawin, J. D. Woollins, *J. Am. Chem. Soc.* **2010**, *132*, 5799–5802.
[38] L.-C. Song, J.-H. Ge, X.-G. Zhang, Y. Liu, Q.-M. Hu, *Eur. J. Inorg. Chem.* **2006**, 3204–3210.
[39] J. D. Lawrence, H. Li, T. B. Rauchfuss, M. Bénard, M.-M. Rohmer, *Angew. Chem.* **2001**, *113*, 1818; *Angew. Chem. Int. Ed.* **2001**, *40*, 1768–1771.
[40] L.-C. Song, J.-H. Ge, X.-F. Liu, L.-Q. Zhao, Q.-M. Hu, *J. Organomet. Chem.* **2006**, *691*, 5701–5709.
[41] R. A. Kipp, J. A. Simon, M. Beggs, H. E. Ensley, R. H. Schmehl, *J. Phys. Chem. A* **1998**, *102*, 5659–5664.
[42] D. González-Rodríguez, C. G. Claessens, T. Torres, S. Liu, L. Echegoyen, N. Vila, S. Nonell, *Chem. Eur. J.* **2005**, *11*, 3881–3893.
[43] J.-Y. Liu, H.-S. Yeung, W. Xu, X. Li, D. K. P. Ng, *Org. Lett.* **2008**, *10*, 5421–5424.
[44] D. González-Rodríguez, E. Carbonell, G. de M. Rojas, C. A. Castellanos, D. M. Guldi, T. Torres, *J. Am. Chem. Soc.* **2010**, *132*, 16488–16500.
[45] B. del Rey, T. Torres, *Tetrahedron Lett.* **1997**, *38*, 5351–5354.
[46] H. Ozawa, M. Haga, K. Sakai, *J. Am. Chem. Soc.* **2006**, *128*, 4926–4927.
[47] S. Rau, D. Walther, J. G. Vos, *Dalton Trans.* **2007**, 915–919.
[48] A. Fihri, V. Artero, M. Razavet, C. Baffert, W. Leibl, M. Fontecave, *Angew. Chem.* **2008**, *120*, 574; *Angew. Chem. Int. Ed.* **2008**, *47*, 564–567.
[49] J. Rosenthal, J. Bachman, J. L. Dempsey, A. J. Esswein, T. G. Gray, J. M. Hodgkiss, D. R. Manke, T. D. Luckett, B. J. Pistorio, A. S. Veige, D. G. Nocera, *Coord. Chem. Rev.* **2005**, *249*, 1316–1326.
[50] Y. Amao, Y. Tomonou, Y. Ishikawa, I. Okura, *Int. J. Hydrogen Energy* **2002**, *27*, 621–625.
[51] L.-C. Song, L.-X. Wang, G.-J. Jia, Q.-L. Li, J.-B. Ming, *Organometallics* **2012**, *31*, 5081–5088.
[52] A. Weitemeyer, H. Kliesch, D. Wöhrle, *J. Org. Chem.* **1995**, *60*, 4900–4904.
[53] D. Seyferth, R. S. Henderson, L.-C. Song, *Organometallics* **1982**, *1*, 125–133.
[54] *CRYSTALCLEAR*, v. 1.3.6, Rigaku, The Woodlands, **2005**.
[55] G. M. Sheldrick, *SADABS*, *A Program for Empirical Absorption Correction of Area Detector Data*, University of Göttingen, Germany, **1996**.
[56] G. M. Sheldrick, *SHELXS97*, *A Program for Crystal Structure Solution*, University of Göttingen, Germany, **1997**.
[57] G. M. Sheldrick, *SHELXL97*, *A Program for Crystal Structure Refinement*, University of Göttingen, Germany, **1997**.

Received: January 13, 2013
Published Online: March 26, 2013

 